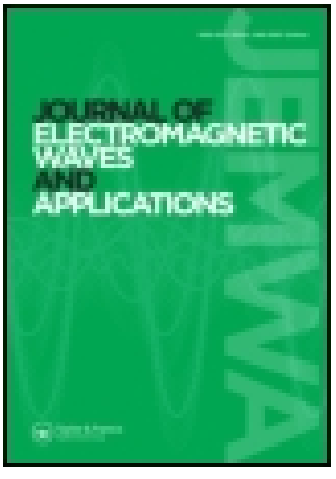

Journal of Electromagnetic Waves and Applications

Publication details, including instructions for authors and subscription information:
http://www.tandfonline.com/loi/tewa20

Evaluating the top electrode voltage distribution uniformity in radio frequency systems

K. Wang[a], L. Chen[a], W. Li[a] & S. Wang[ab]

[a] College of Mechanical and Electronic Engineering, Northwest A&F University, Yangling, Shaanxi 712100, China

[b] Department of Biological Systems Engineering, Washington State University, Pullman, WA 99164-6120, USA

Published online: 16 Mar 2015.

To cite this article: K. Wang, L. Chen, W. Li & S. Wang (2015): Evaluating the top electrode voltage distribution uniformity in radio frequency systems, Journal of Electromagnetic Waves and Applications, DOI: 10.1080/09205071.2015.1021018

To link to this article: http://dx.doi.org/10.1080/09205071.2015.1021018

Journal of Electromagnetic Waves and Applications, 2015
http://dx.doi.org/10.1080/09205071.2015.1021018

Taylor & Francis
Taylor & Francis Group

Evaluating the top electrode voltage distribution uniformity in radio frequency systems

K. Wang[a], L. Chen[a], W. Li[a] and S. Wang[a,b]*

[a]*College of Mechanical and Electronic Engineering, Northwest A&F University, Yangling, Shaanxi 712100, China;* [b]*Department of Biological Systems Engineering, Washington State University, Pullman, WA 99164-6120, USA*

(*Received 25 November 2014; accepted 16 February 2015*)

Studies on the voltage distribution on the top electrode are important to improve the radio frequency (RF) heating uniformity of samples. The goal of this study was to evaluate the top electrode voltage distribution uniformity in RF systems. The voltages of five representative points on the top electrode were measured by a measuring device with 3 kg soybeans, and validated by the heating patterns using 0.9 kg soybeans located at five positions of the RF cavity. The results showed that the length effect of the copper straps used for connecting the measuring points and measuring device should be taken into account by ignoring little effects of the strap shapes. The final voltages away from the feed strip were higher than those near the feed strip and the deviations between the minimum and the maximum values among the five voltages were 694.3 and 440.9 V, corresponding to the highest voltage difference of 11.99 and 7.12% without and with load, respectively. The real top electrode voltage distribution could be potentially used in computer simulations to achieve the accurate RF heating patterns.

Keywords: RF; top electrode voltage; distribution uniformity; copper strap; soybean

1. Introduction

As a member of the electromagnetic spectrum, radio frequency (RF) with a frequency range of 3 kHz to 300 MHz has been increasingly studied in recent years. RF heating has been applied in agricultural products and food processing fields as an efficient dielectric heating method for years because of its rapid and volumetric heating, large power penetration depth, and high energy efficiency.[1–3] Successful commercial RF heating applications have been used in thawing [4,5] and post baking.[6,7] Many of the RF systems have been extensively used in laboratory studies for disinfestation,[8–14] drying,[15–17] tissue heating,[18,19] and pasteurization.[20,21] The free-running oscillator RF system with parallel plate electrodes is still the most commonly used in the food industry because of the low cost, simple structure, and flexibility.[1] Sensitivity analyses in the computer simulation of RF heating show that the voltage of the top electrode is an important index to influence the electromagnetic field intensity and final temperature in samples and needs to be determined.[22,23] The recently developed measurement system [24] provides a practical and repeatable method to quickly determine the top electrode voltage of the RF system.

*Corresponding author. Email: shaojinwang@nwsuaf.edu.cn

In the past studies, the voltage is assumed to be uniformly distributed over the top electrode because the dimensions of the top electrode are designed to be less than 30% of the RF wavelength (11 m) at 27.12 MHz.[25] For example, a single and uniform top electrode voltage was applied to simulate the temperature distributions in various RF-treated agricultural and food products.[22,23,26–30] In reality, the voltage varies all over the surface of the top electrode, since it has the minimum value at the feed point and increases to a maximum value when reaching the electrode edge far away from the feed point.[23,31] The different RF heating uniformity has been reported in seven foam sheets located at different positions under the top electrode, suggesting that the electric field at the far end of the electrode would be higher than that close to the feed point.[32] The heating uniformity in RF-treated polyurethane foams or water loads could be improved after the symmetric design of feeding and inductance positions on the top electrode.[33] It is desirable to determine the top electrode voltage distribution in the RF systems for further improving the heating uniformity of samples.

The objectives of this research were to: (1) determine the effect of the connection copper strap shape and length of the measurement system on the output voltage, (2) measure the voltages of the five representative points on the top electrode, and (3) validate the top electrode voltage distribution based on heating patterns of 0.9 kg soybeans located at five positions of the RF cavity.

2. Materials and methods

2.1. *Materials and RF heating systems*

Soybeans (Glycine max) were purchased from a local supermarket in Yangling, Shaanxi, China. The original moisture content of soybeans was 8.7% on wet basis (w.b.). Before each test, samples were placed in an incubator (BSC-150, Boxun Industry & Commerce Co., Ltd, Shanghai, China) for 12 h at 25 ± 0.5 °C for equilibrium.

A 6 kW, 27.12 MHz free-running oscillator pilot-scale RF heating system (SO6B, Strayfield International, Wokingham, UK) was used to study the top electrode voltage distribution (Figure 1). This applicator system had two parallel plate electrodes. The size of top electrode was 400 mm (W) × 830 mm (L), and the feed strip was located at the middle of the backside on the top electrode plate (Figure 2). Samples were heated between the two electrodes. The gap between the two electrodes was adjusted to have different RF power coupled to the samples.[14] Before the tests, the distance between the top and bottom electrode plates was adjusted to be constant (variation < 1 mm) over

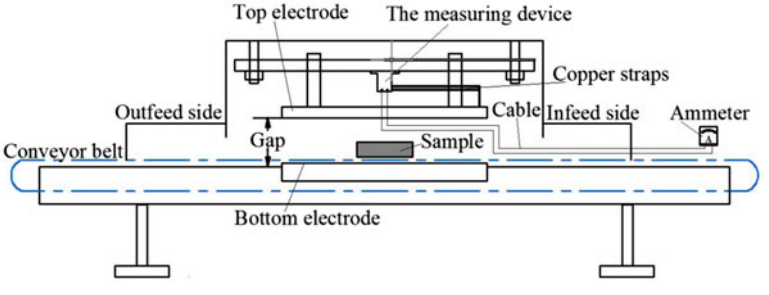

Figure 1. Schematic view of the pilot-scale 6 kW, 27.12 MHz RF unit showing the measuring device, and copper straps.[14]

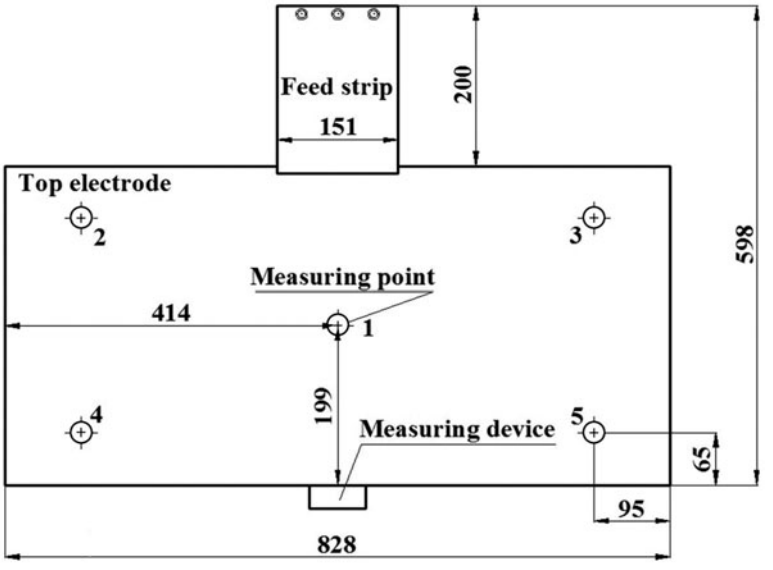

Figure 2. Schematic view of the positions of feed strip, measuring device, and measuring points on the top electrode (all dimensions are in mm).

the entire electrode plate surface to avoid the effect of gap variations between the electrode plates on the electromagnetic field.[33]

2.2. *Experimental determination of the voltage distribution on top electrode*

2.2.1. *The measuring device*

A measuring device designed in a previous study [24] was used to directly measure the top electrode voltage. The connection between the top electrode plate and measuring

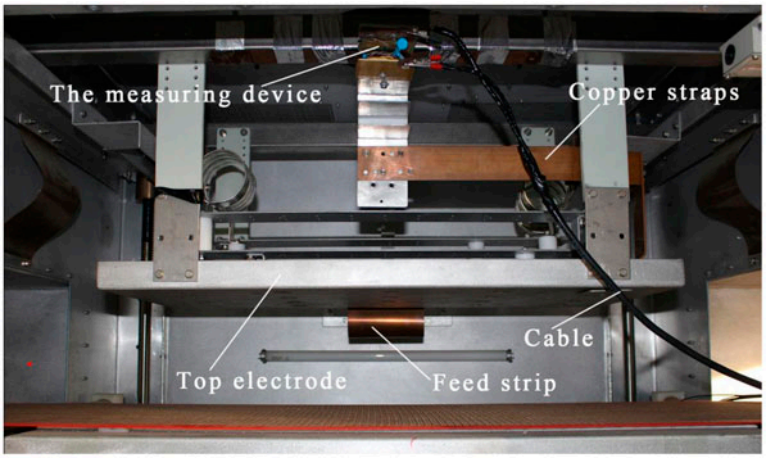

Figure 3. Arrangement of the measuring device and copper straps in the RF heating cavity.

device (Figures 1 and 3) was made by copper straps (3 mm H × 50 mm W), which have the particularly designed shape and length. The major part of the measuring device was fixed on the frame above the top electrode plate and grounded well (Figure 3), but the ammeter was located outside the RF cavity (Figure 1) to prevent interference from the high electromagnetic field intensity. A well-shielding cable was used to connect the two parts of the measuring device.[24]

Before the RF heating test, the measuring device and the selected measuring points were connected by the particularly designed copper straps. The electric circuit of the measuring device was shown in Figure 4, which mainly consisted of voltage divider, filter, and measuring parts.[24] During the RF heating under the given conditions, the electrical current (A) was recorded from the ammeter and converted into the top electrode voltage using the corresponding relationship developed in a previous study.[24]

The measuring space above the top electrode was limited due to feed connections and inductance tuning distributions, indicating that the connection between measuring points and the measuring device must be designed properly. To determine the effect of the connecting strap on the measured voltage at various locations, the copper straps were specifically designed in different shapes and lengths. The connecting part was polished to avoid the effect of oxide on possible conductivity changes. Before the multipoint measurement tests, the relationship between the output voltage and the copper strap shape and length should be determined.

2.2.2. *The voltage measurement in the same point with different copper strap shapes*

Samples were removed from the incubator immediately to have a uniform initial temperature (25 °C) prior to RF heating. The 3 kg soybean samples in a polypropylene container (300 mm L × 220 mm W × 85 mm H) with perforated side and bottom walls were placed on the center of the bottom electrode, the height of soybeans in the container was 60 mm. The RF heating was conducted at the electrode gap of 120 mm without the conveyor belt movement, and this gap was determined from the previous study to obtain appropriate heating rates in soybean samples.[24] The container was supported on two slim bars (200 mm L × 30 mm W × 30 mm H) made of polyurethane, to raise the sample bottom by 30 mm above the bottom electrode, so the samples were in the middle between the top and bottom electrodes.

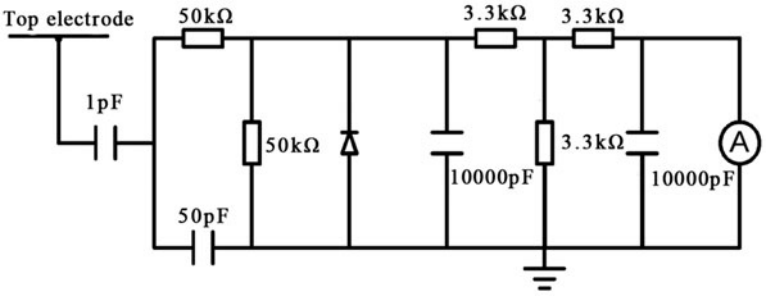

Figure 4. The electric circuit for measuring the current from top electrode of the RF system.[24]

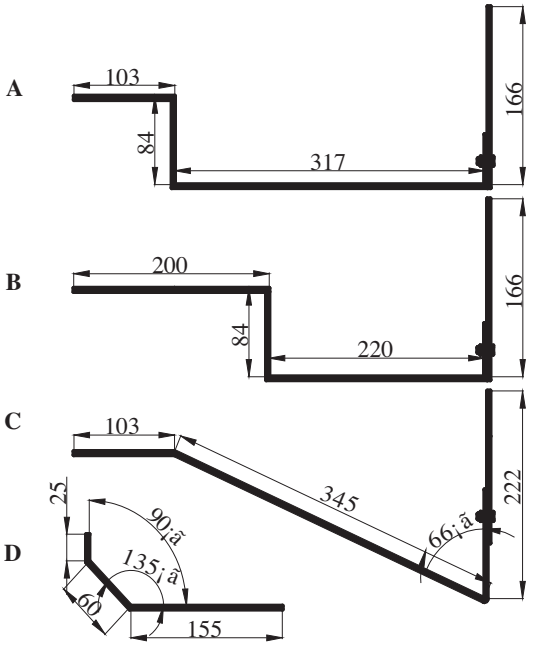

Figure 5. Three shapes of copper straps (A+D, B+D, C+D) for measuring the voltage of point 5 (all dimensions are in mm).

To explore the relationship between the output voltage and the copper strap shape, three pieces of equal length copper straps were processed into three shapes (Parts A, B, and C) together with the core part D, as shown in Figure 5. Considering the connection part at both ends of the copper straps, the total length between the measuring point and the measuring device was 817 mm for all three shapes. The voltage at point 5 (Figure 2) was measured with three replicates. *T*-test was used to analyze the difference of three mean values. The measured currents were read from the ammeter after reaching the stability. After the reading, the RF unit was turned off and each of three copper strap shapes was changed one by one. Three decimal point readings were required to ensure the measurement accuracy of the current value. Based on the measured currents (I_m, A) observed above, the voltages (V, V) at the point 5 were estimated by the following equation developed by Zhu et al. [24]:

$$V = -22760 \times I_m + 7384.2 \tag{1}$$

2.2.3. *The voltage measurement in the same point with different copper strap lengths*

Since the effect of copper strap shapes on the voltage was negligible based on the results above, four possible lengths of 617, 705, 817, and 978 mm were selected to measure the top electrode voltages at point 5 (Figure 2). The measured currents were obtained when 3 kg soybeans with the moisture content of 8.7% in the container were heated at the electrode gap of 120 mm. All other procedures were the same as described in the above section. Each test was repeated three times. The measured voltage as a function of the strap length could be developed for further comparisons at different positions.

2.2.4. The multipoints measurement of the top electrode voltage

To study the voltage distribution over the entire top electrode plate, five representative points (Figure 2) were selected for measuring the top electrode voltage using the developed measuring device. Five kinds of copper straps with different lengths (380 mm for P1 and 817 mm for P2–P5) were designed to connect the measuring points and the measuring device. All other procedures were the same as described above. Each test was repeated three times. The correlation between the voltage and the length developed above was further used to calibrate and compare the measured voltage based on a same length.

2.3. Validation of the voltage distribution using RF heating patterns

To validate the measured top electrode voltage distribution uniformity, RF heating uniformity tests were conducted with a sample container located below the five points of voltage measurements without the conveyor belt movement. About 0.9 kg soybeans with the moisture content of 8.7% (w.b.) were filled in this polypropylene container (197 mm L × 98 mm W × 60 mm H) with perforated side and bottom walls. The soybeans in the container were divided into three layers and separated by two thin gauzes (with mesh opening of 1 mm) to easily map the sample temperatures at heights of 20, 40, and 60 mm after RF treatments. The container was placed at each of the five positions on the bottom electrode (Figure 6), which were corresponding to the five measuring points on the top electrode in Figure 2. The container was supported on two slim bars (110 mm L × 30 mm W × 30 mm H) to raise the sample bottom by 30 mm above the bottom electrode. Thus, the samples were located in the middle section between the top and bottom electrodes with the electrode gap of 120 mm. The RF unit was turned off after 4.1 min treatments to achieve about 52 °C of the average sample temperature in the middle layer at position 1 determined in the preliminary experiment.

After the RF heating was stopped, the container was immediately moved out for the surface temperature measurement. The surface temperatures were measured with a digital infrared camera (DM63, Dali Science and Technology, Hangzhou, Zhejiang, China) with an accuracy of ±2 °C, which was obtained after calibrations against a thermocouple thermometer (HH-25TC, Type-T, OMEGA Engineering Inc., Stamford, Connecticut, USA) with an accuracy of ±0.5 °C. Details on measurement procedure and the precision of this type of camera can be found elsewhere.[12,14,24,34,35] Thermal images were taken for the upper surface of soybeans, beginning with the top layer

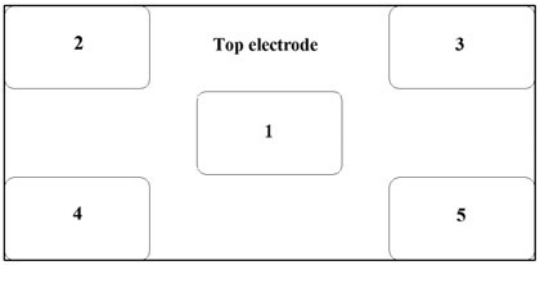

Figure 6. Distribution of five locations for RF heating uniformity tests with a load of 0.9 kg soybeans at the moisture content of 8.7% (w.b.).

working toward the bottom one. The total measurement time for the three layers was about 15 s. From each of the thermal images, 16,228 individual surface temperature data points were collected over a sample surface in the container and used for statistical analyses.[13,17,36] The average surface temperatures and standard deviations for each layer were calculated. Each test was repeated three times.

3. Results and analyses

3.1. Relationship between the output voltage and the copper strap shape

The voltages of point 5 (Figure 2) determined by three-shape copper straps with the same total length are shown in Table 1. The voltage value for each shape was repeatable due to small standard deviations over three replicates. The mean voltages from three shapes were not significantly different ($p > 0.05$), suggesting that the change of the copper strap shape with the same length did not affect the output voltage of the top electrode.

3.2. Relationship between the output voltage and the copper strap length

The voltages as a function of the length of the copper strap with and without 3 kg soybeans at the moisture content of 8.7% (w.b.) are shown in Figure 7. The top electrode voltage was clearly influenced by the length of the copper strap. The output voltage increased linearly with increasing the length of the copper strap. The regression equations were fitted with high coefficient of determination (>0.98) both with and without the load. These regression equations were further used to correct the voltage measured from the five representative positions (Figure 2). Based on the length correction ratios (R_1 = 1.73 V/mm without load and R_2 = 1.43 V/mm with load) obtained from Figure 7, the voltages of other four representative points were calibrated based on that at the central position (P1) by the following equation:

$$V_F = V_R - (L_2 - L_1) \cdot R_i \tag{2}$$

where V_F is the final voltage after calibration (V, V), V_R is the relative voltage before calibration (V, V), L_2 is length of the copper straps for P2–P5 (817 mm), L_1 is the length of the copper straps for P1 (380 mm), R_i is the coefficient of correction (V/mm, $i = 1$ without load, and $i = 2$ with load).

Table 1. The top electrode voltages of point 5 (Figure 2) as influenced by copper strap shapes.

Shape with the same total length (817 mm)	Voltage for three replicates (V)			Mean ± SD
	1	2	3	
A + D	7202.1	7179.4	7111.1	7164.2 ± 47.4a*
B + D	7111.1	7088.3	7111.1	7103.5 ± 13.2a
C + D	7202.1	7156.6	7156.6	7171.8 ± 26.3a

*Mean values followed by the same letters within the column are not significantly different ($p > 0.05$).

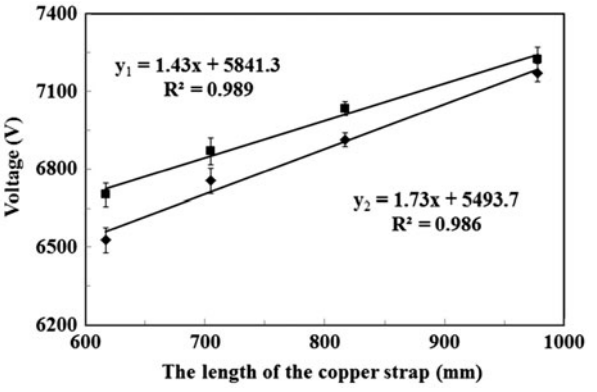

Figure 7. The voltage as a function of the length of the copper straps without (◆) and with (■) 3 kg soybeans at the moisture content of 8.7% (w.b.).

3.3. *Voltage distribution on the top electrode*

The final top electrode voltages of five positions with and without 3 kg soybeans at the moisture content of 8.7% (w.b.) after strap length calibrations are listed in Table 2. Generally, the voltages at P4 and P5 were higher than those at P2, P3, and P1, suggesting that the voltage away from the feed point was higher than that near the feed point (Figure 2). This distribution behavior of the top electrode voltage was in good agreement with results in similar RF heating systems reported by Tiwari et al. [23] and Wang et al. [37,38]. The electromagnetic wave travelled from the feeding point to the far end of the electrode,[32] resulting in low voltages at the feeding point and the relatively high intense electric field at the far end of the electrode (P4 and P5).

Specifically, the deviations between the minimum and the maximum values among the five voltages were 694.3 and 440.9 V, corresponding to the highest voltage difference of 11.99 and 7.12% without and with load, respectively. The voltage was the lowest at the central position (P1), where the samples were usually placed in the past studies. The average deviation of voltages over five positions between with load and without load was 6.1%, which was in agreement with the voltage variation of only 7% between standbys and full load for a typical industrial-scale RF system reported by Metaxas [39]. If moving the feeding point to the geometry center of the top electrode, the current voltage difference would be greatly reduced.

Table 2. Values (Mean ± SD) of the measured top electrode voltage in the five positions with and without 3 kg soybeans at the moisture content of 8.7% (w.b.) after strap length calibrations.

	Positions				
Voltage (V)	P1	P2	P3	P4	P5
Without load	5791.0 ± 45.5	6028.9 ± 47.4	5839.2 ± 52.6	6370.3 ± 69.5	6332.3 ± 60.2
With load	6193.1 ± 34.8	6288.1 ± 26.3	6204.7 ± 13.1	6576.4 ± 22.8	6530.9 ± 5.5

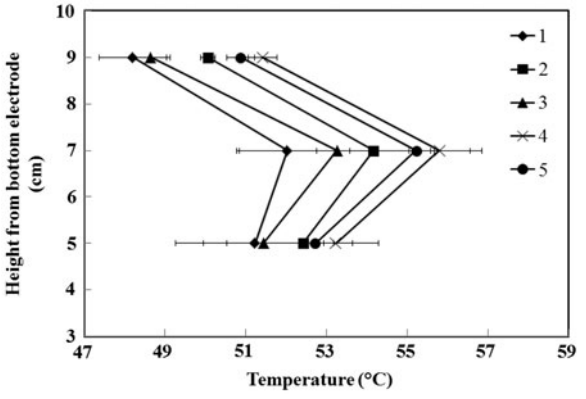

Figure 8. Surface temperature (Mean ± SD) profiles as a function of height of soybean (0.9 kg) layers at five positions after 4.1 min RF heating under an electrode gap of 120 mm.

3.4. Voltage distribution validation based on RF heating patterns

Figure 8 shows the surface temperature (Mean ± SD) profiles as a function of height of soybean layers after 0.9 kg soybeans were RF heated for 4.1 min at an electrode gap of 120 mm at five positions. Due to heat losses to the ambient air and the bottom container, the sample temperatures at the top and bottom layers were lower than those at middle layers, which were also observed in RF-heated foams.[12,38] Generally, the average surface temperatures at five positions followed the same order in each of three layers. Especially, the average surface temperatures at P4 and P5 were higher than those at P2, P3, and P1, which had a similar order to the five voltages listed in Table 2. The similar sample temperature distribution was also observed at different positions of the RF cavity.[39] This study further confirmed that the higher voltage at specific locations of the top electrode resulted in higher local sample temperatures. The obtained results suggested that the required RF uniform heating could be first achieved by improving the top electrode voltage distribution.

4. Conclusion

The output voltage of the RF systems was not influenced by the copper strap shape connected to the measuring device, but increased linearly with increasing the length of the copper strap. The absolute top electrode voltages were determined at five representative points after calibration of the copper strap lengths. The final voltages away from the feed strip were higher than those near the feed strip, since the electromagnetic wave travelled from the feeding to the electrode edge. The deviations between the minimum and the maximum values among the five voltages were 694.3 and 440.9 V without and with load, respectively. The voltage distribution behavior on the top electrode was validated by the heating patterns of 0.9 kg soybeans placed in the five positions of the RF cavity. Further studies could be conducted to improve the RF heating uniformity by appropriately locating the feed strip and inductance positions.

Acknowledgements

We gratefully thank Hankun Zhu, Zhi Huang, Rongjun Yan, Bo Ling, Lixia Hou, and Rui Li for their helps on data processing and suggestions to improve experimental design.

Funding

This research was conducted in College of Mechanical and Electronic Engineering, Northwest A&F University, Yangling, China and supported by research grants from PhD Programs Foundation of Ministry of Education in China [grant number 20120204110022]; Program of Introducing International Advanced Agricultural Science and Technologies (948 Program) of Ministry of Agriculture of China [grant number 2014-Z21]; General Program of National Natural Science Foundation in China [grant number 31371853].

References

[1] Jiao Y, Tang J, Wang S, Koral T. Influence of dielectric properties on the heating rate in free-running oscillator radio frequency systems. J. Food Eng. 2014;120:197–203.
[2] Liu Y, Yang B, Mao Z. Radio frequency technology and its application in agro-product and food processing. Trans. CSAE. 2010;41:115–120.
[3] Piyasena P, Dussault C, Koutchma T, Ramaswamy HS, Awuah GB. Radio frequency heating of foods: principles, applications and related properties – a review. Crit. Rev. Food Sci. 2003;43:587–606.
[4] Farag KW, Lyng JG, Morgan DJ, Cronin DA. Dielectric and thermophysical properties of different beef meat blends over a temperature range of −18 to +10°C. Meat Sci. 2008;79:740–747.
[5] Farag KW, Lyng JG, Morgan DJ, Cronin DA. A comparison of conventional and radio frequency thawing of beef meats: effects on product temperature distribution. Food Bioprocess Technol. 2011;4:1128–1136.
[6] Koral T. Radio frequency heating and post-baking. Biscuit World Iss. 2004;7:1–6. Available from: http://www.strayfield.co.uk/images/radio_frequency.pdf
[7] Koray Palazoğlu T, Coşkun Y, Kocadağlı T, Gökmen V. Effect of radio frequency postdrying of partially baked cookies on acrylamide content, texture, and color of the final product. J. Food Sci. 2012;77:E113–E117.
[8] Jiao S, Johnson JA, Tang J, Wang S. Industrial-scale radio frequency treatments for insect control in lentils. J. Stored Prod. Res. 2012;48:143–148.
[9] Lagunas-Solar M, Pan Z, Zeng N, Truong T, Khir R, Amaratunga K. Application of radio-frequency power for non-chemical disinfestation of rough rice with full retention of quality attributes. Appl. Eng. Agric. 2007;23:647.
[10] Shrestha B, Baik O-D. Radio frequency selective heating of stored-grain insects at 27.12 MHz: a feasibility study. Biosyst. Eng. 2013;114:195–204.
[11] Tang J, Ikediala J, Wang S, Hansen JD, Cavalieri R. High-temperature-short-time thermal quarantine methods. Postharvest Biol. Technol. 2000;21:129–145.
[12] Wang S, Monzon M, Johnson JA, Mitcham EJ, Tang J. Industrial-scale radio frequency treatments for insect control in walnuts. Postharvest Biol. Technol. 2007;45:240–246.
[13] Wang S, Monzon M, Johnson JA, Mitcham EJ, Tang J. Industrial-scale radio frequency treatments for insect control in walnuts. Postharvest Biol. Technol. 2007;45:247–253.
[14] Wang S, Tiwari G, Jiao S, Johnson JA, Tang J. Developing postharvest disinfestation treatments for legumes using radio frequency energy. Biosyst. Eng. 2010;105:341–349.
[15] Lee N-H, Li C, Zhao X-F, Park M-J. Effect of pretreatment with high temperature and low humidity on drying time and prevention of checking during radio-frequency/vacuum drying of Japanese cedar pillar. J. Wood Sci. 2009;56:19–24.
[16] Marshall MG, Metaxas AC. Radio frequency assisted heat pump drying of crushed brick. Appl. Therm. Eng. 1999;19:375–388.
[17] Wang Y, Zhang L, Johnson J, Gao M, Tang J, Powers JR, Wang S. Developing hot air-assisted radio frequency drying for in-shell macadamia nuts. Food Bioprocess Technol. 2013;7:278–288.
[18] Rajhi A. Optimization of the EM heating cycle by using a dual frequency local hyperthermiaapplicator. J. Electromagn. Waves Appl. 2003;17:447–464.
[19] Mohsin SA, Sheikh NM, Abbas W. MRI induced heating of artificial bone implants. J. Electromagn. Waves Appl. 2009;23:799–808.

[20] Gao M, Tang J, Villa-Rojas R, Wang Y, Wang S. Pasteurization process development for controlling Salmonella in in-shell almonds using radio frequency energy. J. Food Eng. 2011;104:299–306.
[21] Kim SY, Sagong HG, Choi SH, Ryu S, Kang DH. Radio-frequency heating to inactivate Salmonella Typhimurium and Escherichia coli O157:H7 on black and red pepper spice. Int. J. Food Microbiol. 2012;153:171–175.
[22] Alfaifi B, Tang J, Jiao Y, Wang S, Rasco B, Jiao S, Sablani S. Radio frequency disinfestation treatments for dried fruit: model development and validation. J. Food Eng. 2014;120:268–276.
[23] Tiwari G, Wang S, Tang J, Birla SL. Computer simulation model development and validation for radio frequency (RF) heating of dry food materials. J. Food Eng. 2011;105:48–55.
[24] Zhu H, Huang Z, Wang S. Experimental and simulated top electrode voltage in free-running oscillator radio frequency systems. J. Electromagn. Wave. Appl. 2014;28:606–617.
[25] Barber H. Electroheat. London: Granada; 1983.
[26] Birla SL, Wang S, Tang J. Computer simulation of radio frequency heating of model fruit immersed in water. J. Food Eng. 2008;84:270–280.
[27] Huang Z, Zhu H, Yan R, Wang S. Simulation and prediction of radio frequency heating in dry soybeans. Biosyst. Eng. 2015;129:34–47.
[28] Marshall MG, Metaxas AC. Modeling of the radio frequency electric field strength developed during the RF assisted heat pump drying of particulaates. J. Microwave Power Electromagn. Energy. 1998;33:167–177.
[29] Marra F, Lyng J, Romano V, McKenna B. Radio-frequency heating of foodstuff: solution and validation of a mathematical model. J. Food Eng. 2007;79:998–1006.
[30] Tiwari G, Wang S, Tang J, Birla SL. Analysis of radio frequency (RF) power distribution in dry food materials. J. Food Eng. 2011;104:548–556.
[31] Uyar R, Erdogdu F, Marra F. Effect of load volume on power absorption and temperature evolution during radio-frequency heating of meat cubes: a computational study. Food Bioprocess Technol. 2014;92:243–251.
[32] Orfeuil M. Electric process heating: technologies, equipment, applications. Columbus (OH): Battelle Press; 1987.
[33] Wang S, Luechapattanaporn K, Tang J. Experimental methods for evaluating heating uniformity in radio frequency systems. Biosyst. Eng. 2008;100:58–65.
[34] Tiwari G, Wang S, Birla S, Tang J. Effect of water-assisted radio frequency heat treatment on the quality of 'Fuyu'persimmons. Biosyst. Eng. 2008;100:227–234.
[35] Wang S, Birla SL, Tang J, Hansen JD. Postharvest treatment to control codling moth in fresh apples using water assisted radio frequency heating. Postharvest Biol. Technol. 2006;40:89–96.
[36] Wang S, Yue J, Tang J, Chen B. Mathematical modelling of heating uniformity for in-shell walnuts subjected to radio frequency treatments with intermittent stirrings. Postharvest Biol. Technol. 2005;35:97–107.
[37] Wang Y, Li Y, Wang S, Zhang L, Gao M, Tang J. Review of dielectric drying of foods and agricultural products. Int. J. Agric. Biol. Eng. 2011;4:1–19.
[38] Wang Y, Zhang L, Gao M, Tang J, Wang S. Evaluating radio frequency heating uniformity using polyurethane foams. J. Food Eng. 2014;136:28–33.
[39] Metaxas A. Foundations of electroheat: a unified approach. Chichester (UK): Wiley; 1996.